

Chemisorption of Na on the Ti Nanoparticle surface and its effects on the Na-H₂O reaction reactivity

Soo Jae Kim^{a,b*}, Gunyeop Park^a, Hyun Sun Park^c, Moo Hwan Kim^d, Jehyun Baek^a

^aDepartment of Mechanical Engineering, POSTECH, Pohang, Gyungbuk 790-784, Republic of Korea

^bKorea Atomic Energy Research Institute, Yuseong, Daejeon, 305-353, Republic of Korea

^cDivision of Advanced Nuclear Engineering, POSTECH, Pohang, Gyungbuk 790-784, Republic of Korea

^dKorea institute of Nuclear Safety, Yuseong, Daejeon 305-338, Republic of Korea

*Corresponding author: ksj0530@kaeri.re.kr

1. Introduction

Sodium water reaction (SWR) has been a safety issue on the Sodium Fast cooled Reactor (SFR). when Na comes into direct contact with water or moist air, a violent exothermic sodium-water reaction (SWR) rapidly releases a large amount of heat and gases including explosive H₂ and corrosive NaOH. In 1995, an Na leakage accident occurred at the Monju reactor in Japan; the Na leaked from a pipe and reacted with water; the resulting intense fire warped some steel structures. This accident showed that elimination of SWR risk should be one of the most significant design criteria for the development of safe SFRs. Design solutions to ensure isolation of the Na from the water have been proposed; these include double-walled structures in the steam generator and at coolant boundaries[1–3]and guard vessels or guard piping lines filled with inert gas[2]. However, those methods cannot be ultimate solutions because the system still has a possibility of failure.

An alternative approach to reduce the severity of the SWR is to reduce the reactivity of Na. Recently, this goal has been achieved by suspending a small amount of Ti nanoparticles (NPs) in liquid Na. Adding 2 at% of 10-nm Ti NPs in liquid Na reduced the heat of the reaction up to 80% and H₂ production rate by 10% [4–6]. Addition of 0.21 vol % Ti NP (< 100 nm) to liquid Na reduced the SWR reaction rate by up to 50% [7–9].

A strong atomic interaction between Na atoms and Ti NPs surface has been insisted as a key mechanism [6,10,11]; Recent study has found Na atoms were adsorbed on to Ti NPs surface and its strength was 1.6eV by using Ab-initio calculation[10]. However, the exact relation between Na adsorption and SWR reactivity has not been modeled yet; If SWR reactivity reduction is achieved by Na adsorption, knowing the number of the adsorbed Na atoms on the Ti Nps surface will be essential to develop the model.

Therefore, the number of adsorbed Na atoms onto Ti NPs with respect to the various temperature and pressure was calculated by using ab-initio and thermodynamics. Furthermore, the model which relates the Na chemisorption and SWR reactivity was proposed.

2. Chemisorption of Na onto Ti NPs surface

Chemisorption is caused by a chemical bond between atoms from adsorbents and the surface. The strength of the chemisorption is relatively stronger than physical adsorption, and often has activation energy. The reactant's electron structure changes in most chemical reactions; Chemically-adsorbed Na atoms have different electron structure than Na atoms in a bulk liquid Na; therefore the reaction between adsorbed Na and H₂O is different from the SWR.

In this study, chemisorption energy E_{ads} and the electronic state of Na on a Ti NP surface were studied. To determine the most stable states of adsorbed Na, ab-initio calculation was conducted at four adsorption sites (top, bridge, fcc hollow, hcp hollow) and three Na coverages (1ML, 0.5ML, 0.25ML). In addition, temperature and pressure effects on the adsorption were modeled using ab-initio thermodynamics. The calculation results were validated by existing experimental results.

2.1 Ab-initio calculation method

Chemical adsorption causes electron structure change, so the Schrödinger equation should be solved to describe chemical adsorption exactly. The time-independent Schrödinger equation of a system composed of many nuclei and electrons is

$$(T_N + U_{N-N} + T_e + U_{e-e} + U_{N-e})\Psi(R, r) = E\Psi(R, r) \quad (1)$$

The ground state electron wave function within a fixed nucleus position can be obtained by using the Born-Oppenheimer approximation[12]

$$(T_e + U_{e-e} + U_{N-e})\Psi(r) = E\Psi(r) \quad (2)$$

To adhere to the Pauli principle, the Slater determinant[13] is often used to describe the wave function of many electron system; most systems consist of many electrons and therefore eq (2) is difficult to solve directly. The complexity caused by interaction among many electrons can be removed by solving the Kohn-Sham equation.

$$(T_{e,non-int} + U_{KS}(n(r)))\phi_i(r) = \varepsilon_i\phi_i(r) \quad (3)$$

Where,

$$T_{e,non-int} = -\frac{\hbar}{2m}\nabla^2, U_{KS}(n(r)) = U_{ext} + U_H + U_{xc} \quad (4)$$

In the Kohn-Sham equation, a system Hamiltonian can be mapped on to kinetic energy of non-interacting

electrons and effective potential energy by using Hohenberg-Kohn theorems[14] and the Kohn-Sham ansatz [15]. The total energy E of the system can be a function of an electron ground state number density

$$n(r) = \sum_{i=1}^{N_{occ}} |\phi_i(r)|^2, \int n(r) dr = N_{electron} \quad (5)$$

Kohn-Sham potential V_{KS} is composed of external potential V_{ext} caused by a fixed nucleus, Hartree potential V_H due to columbic interaction among electrons, and exchange-correlation potential V_{xc} . V_{xc} indicates kinetic energy difference between a fictitious non interacting electrons and its spin effect on the energy. Not like other potentials, V_{xc} has no exact formula but only has models such as local density approximation (LDA), generalized gradient approximation (GGA), hybrid GGA and meta GGA model. When the system consists of well-ordered atoms such as a solid, a plane-wave basis is often used as basis function to solve the Kohn Sham equation. To reduce the total number of electrons in the system and the size of the high-frequency plane wave basis set, we used the pseudo-potential technique, which considers only valence electrons, which often have major influence on chemical reactions, and regarded the ensembles of core electrons plus nuclei to be ions. Because the effective potential of the Kohn-Sham equation is also a density functional, it should be solved self-consistently. A ground state density can be obtained by using the variational principle and a constraint on the number of electrons. After solving the Kohn-Sham equation, the total energy of the system can be evaluated as

$$E_{total} = E_{KS} = 2 \sum_{i=1}^{N_{electron}/2} \epsilon_i - \frac{1}{2} \int U_H(r) n(r) dr + E_{N-N} \quad (6)$$

Kohn-Sham equation was solved by using Quantum Espresso Package[16], open source solver. We use a plane-wave basis set with 3p3d4s and 2p3s electron structures to model the valence states of Ti and Na atoms, respectively. We used Ultrasoft-pseudo potentials[17] to model the influence of the ensembles of nuclei and core electrons, and set the electron kinetic energy cut off as 816 eV. We used the GGA with PBE functional[18] to model exchange-correlation effects. We neglected relativistic effects.

2.2 Model

An NP surface can have many different arrangements of atoms; thermodynamically the surface with highest atomic density is the most stable [19]; therefore the Ti (0001) surface is used as a target surface in this study.

To model a Ti (0001) surface, a slab of 9 Ti atomic layers is installed and the periodic boundary condition is imposed in the x,y and z directions. The lattice constant of the three Ti atomic layers in the middle of the slab is fixed as the Ti bulk metal lattice constant (2.95 Å) to model the bulk Ti. The other six Ti atomic layers were relaxed in the z direction to model the surface state;

outermost layers were exposed to vacuum. The region between the periodic images in z direction was set > 19 Å to reduce the error induced by the periodic boundary condition. According to the Na adsorption study on the Co(0001), the effect of the atomic reconstruction in the lateral direction is not significant[20]; atomic reconstruction at the surface in the lateral direction was neglected. To remove the dipole moment effect on the system, Na was located at both sides of the slab; the Na atoms were initially located near the outermost Ti atomic layers and were free to move until the total system energy reached the global minimum. To investigate Na adsorption effect on the Ti surface configuration, a surface rumpling factor δ was defined as the distance between the topmost Ti layer and the layer beneath it. H was defined as the normal distance between Na and the topmost Ti atoms on the surface. Surface coverage and adsorption site affects E_{ads} and its bonding character. Therefore calculation was conducted for three cases of surface coverage (0.25ML, 0.5ML, 1ML), at four high-symmetry sites (hcp hollow, fcc hollow, top, bridge) (Fig.1). A Monkhorst-Pack mesh[21] with (13x13x1) k points was used for Brillouin zone integration, and Methfessel-Paxton smearing[22] was used to model the electron density near the Fermi level. For every case, the calculation was performed when the residual force of each relaxed ion as < 0.003 eV/Å, and a convergence test was performed for the number of k points and the cutoff of electron kinetic energy.

To validate our calculation, the lattice constants of bulk Ti, Na and bond length of NaCl molecule were calculated (Table 1); calculation results showed the pseudo potential and exchange correlation used was appropriated. To define chemisorption strength, adsorption energy E_{ads} is defined as

$$E_{ads} = (E_{Na/Ti} - E_{Ti} - N_{Na} E_{Na}) / N_{Na} \quad (7)$$

where $E_{Na/Ti}$, E_{Ti} , and E_{Na} are the total energy of the Ti NP with adsorbed Na, of the corresponding Ti(0001) substrate, and of a free Na atom; N_{Na} is the number of Na atoms.

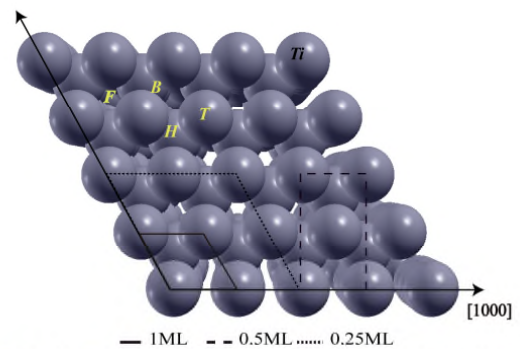


Fig1. Top view of the surface for 3 different unit cells (1ML, 0.5ML, 0.25ML) and 4 different sites (top, bridge, fcc hollow, hcp hollow)

Table 1: Bulk Ti lattice constant and NaCl bond length [\AA]

Target	Calculation	Experiment	Ref
Bulk Ti lattice constant	2.96	2.95	[23]
Bulk Na lattice constant	4.20	4.23	[23]
NaCl bond length	2.37	2.36	[24]

2.3 Ab-initio thermodynamics method

After the ab-initio calculation, the most stable adsorption structure and its bond character can be deduced, however at the expected operation range[25] which is $600 \text{ K} \leq T \leq 900 \text{ K}$, Na is thermally activated; the adsorption will be unstable. The ab-initio calculations were conducted without considering temperature (T) and pressure (P), so to obtain the effects of T and P on the phase stability, an atomistic thermodynamic approach[26,27] was conducted in this study. Originally this approach was based on the assumption that thermodynamic equilibrium between metal surface and a gas such like oxygen was constrained[26], and to obtain the most stable surface phase, surface free energy γ and adsorption surface free energy γ_{ads} were defined as

$$\gamma = \frac{1}{A} (G(T, P, N_{\text{Na}}, N_{\text{Ti}}) - N_{\text{Ti}} g_{\text{Ti}}(T, P) - N_{\text{Na}} g_{\text{Na}}(T, P)) \quad (8)$$

$$\gamma_{\text{clean}} = \frac{1}{A} (G(T, P, 0, N_{\text{Ti}}) - N_{\text{Ti}} g_{\text{Ti}}(T, P)) \quad (9)$$

where $G(g)$, A , N_{Na} and N_{Ti} indicate Gibbs free energy of the system, adsorption surface area, number of Na atoms and Ti atoms respectively.

$$\begin{aligned} \Delta\gamma_{\text{ads}}(T, P) &= \gamma(T, P, N_{\text{Na}}, N_{\text{Ti}}) - \gamma_{\text{clean}}(T, P, 0, N_{\text{Ti}}) \\ &= \frac{1}{A} (G(T, P, N_{\text{Na}}, N_{\text{Ti}}) - G(T, P, 0, N_{\text{Ti}}) - N_{\text{Na}} g_{\text{Na}}(T, P)) \end{aligned} \quad (10)$$

$\Delta\gamma_{\text{ads}}$ indicates the difference between the surface energies of clean surface and adsorbed surface system. At a given combination of T and P, the stability of the phase increases as $\Delta\gamma_{\text{ads}}$ decreases, and $\Delta\gamma_{\text{ads}}=0$ indicates a clean metal surface. To obtain Gibbs free energy, the canonical partition function Q was expanded. Na gas is monoatomic, so the vibrational and rotational partition functions (q_{rot} , q_{vib} respectively) were neglected. In order to remove the volume effects, Na gas was assumed to be ideal gas (no Na-Na interaction); the ideal gas law $PV = Nk_{\text{B}}T$ was used. The Gibbs free energy of Na at specific T and P can be described as

$$\begin{aligned} g_{\text{Na}}(T, P) &\approx -k_{\text{B}}T \ln\left(\frac{(k_{\text{B}}T)^{5/2}}{P} \left(\frac{2\pi m}{h^2}\right)^{3/2}\right) + g_{\text{Na}}^{\text{nuclear\&electrons}} \\ &\approx -k_{\text{B}}T \ln\left(\frac{(k_{\text{B}}T)^{5/2}}{P} \left(\frac{2\pi m}{h^2}\right)^{3/2}\right) + E_{\text{Na}} \end{aligned} \quad (11)$$

where E_{Na} indicates energy from nucleus-nucleus, nucleus-electron, and electron-electron interaction and can be deduced by ab-initio calculation; then

$$\Delta g_{\text{Na}}(T, P) \equiv -k_{\text{B}}T \ln\left(\frac{(k_{\text{B}}T)^{5/2}}{P} \left(\frac{2\pi m}{h^2}\right)^{3/2}\right) \quad (12)$$

represents the effects of T and P. Using the same approach as for Na gas, the Gibbs free energy difference $G(T, p, N_{\text{Na}}, N_{\text{Ti}}) - G(T, p, 0, N_{\text{Ti}})$ between the surfaces can be represented as

$$\begin{aligned} &G(T, P, N_{\text{Na}}, N_{\text{Ti}}) - G(T, P, 0, N_{\text{Ti}}) \\ &\approx E_{\text{Na/Ti}}^{\text{nuclear\&electron}} - E_{\text{Ti}}^{\text{nuclear\&electron}} + TS_{\text{configurational}} \end{aligned} \quad (13)$$

when the difference in vibrational free energies is small. If Na atoms are adsorbed on a clean Ti surface with θ coverage, the maximum configuration entropy will be

$$S_{\text{configurational}} \approx N_{\text{Na}} k_{\text{B}} \left(\ln\left(\frac{1-\theta}{\theta}\right) - \ln(1-\theta)/\theta \right) \quad (14)$$

Substituting Eq.11-14 into Eq.10 yields a definition of $\Delta\gamma_{\text{ads}}$:

$$\begin{aligned} \Delta\gamma_{\text{ads}}(T, P) &= \frac{N_{\text{Na}}}{A} \left[E_{\text{abs}} - \Delta g_{\text{Na}}(T, P) + Tk_{\text{B}} \left(\ln\left(\frac{1-\theta}{\theta}\right) - \ln(1-\theta)/\theta \right) \right] \end{aligned} \quad (15)$$

2.4 Chemisorption strength and its bond character

The stability of a surface increases as its E_{ads} decreases; the hcp hollow site with 0.25ML was the most stable phase in this study (Table 2); this conclusion agrees well with previous results that considered Na adsorption on a transition metal surface [20,28–31]. The absolute E_{ads} decreased with increasing surface coverage because the Na-Na interaction inhibits adsorption. For example when the Ti coverage was 1ML, the absorbed Na-Na distance was 2.9 \AA , which is much shorter than the lattice constant (4.3 \AA) of bulk Na; therefore coulombic repulsion of Na valence electrons will increase the system energy. For each coverage, the hcp hollow site had the lowest E_{ads} among the four adsorption sites tested, because at this site the valence electron of Na has the greatest overlap with the valence electrons of Ti atoms on the surface; i.e., increasing the coordination number increases the stability of adsorption. Surface rumpling δ showed the greatest surface structure relaxation when Na adsorbed to a top site; atomic position reconstruction is not significant due to the adsorption which is same as Na adsorption on other transition metals[20,28–31]. For adsorption to be stable, the topmost Ti atom beneath a Na adatom should be pushed toward the second substrate layer to increase the coordination number.

Na adsorption energies were calculated at the hcp hollow site with 0.25ML for different materials (Table 3). Adsorption energy decreased over the periods; this trend shows how the interaction between Na 3s and metal surface d band affects E_{ads} . Adatom valence state, metal d-band interaction and d-band filling have major effects on E_{ads} [32]. When an adatom approaches the surface, the valence orbitals of adatom and surface atoms overlap; over the periods from 3d to 5d in

transition metals, the surface d band overlap with the valence state of the adatom increases for atoms at given positions. If the d band is sufficiently localized, a bonding orbital and an anti-bonding orbital form[32,33]. If the electron occupies the bonding orbital, the total system energy is decreased, but if the surface has a high d-band filling, the electron can occupy an anti-bonding orbital and thereby increase the total energy. To clarify the bonding character, the projected density of state were plotted for 1 and 0.25ML (Fig. 2). In the 1ML case, 3s states of Na adsorbed on Ti (001) shifted inward to less than Fermi level, but retain a similar shape to that of the 3s state of bulk Na. In contrast, in the 0.25ML case, the Na 3s states became localized and had a resonance peak with the Ti 3d state after adsorption. A strong localized resonance peak between Na 3s and Ti 3d bands below the Fermi level indicates a bonding orbital; a relatively small resonance peak over the Fermi level indicates an anti-bonding orbital. This can explain the high E_{ads} in the 0.25ML coverage; a covalent-metallic bond is made between adsorbed Na and Ti atoms on the Ti NP surface.

2.5 (T,P) diagram of chemisorption

From Eq.15, the most stable adsorption density which had the lowest $\Delta\gamma_{ads}$ for a (T,P) was evaluated. The most stable adsorption density was varied at (T,P). For example, at $T = 300$ K, and $P < 14.7$ MPa, 0.25ML was the most favorable adsorption state and at $P > 14.7$ MPa, 1 ML was the most stable coverage (Fig. 3). However, at $T = 600$ K, only 0.25ML was the most stable and at $T = 1200$ K, Na does adsorbed to the Ti NP surface at all. A phase diagram (Fig. 3) that indicates the dependency of the most stable Na adsorption state with respect to T and P can be used to identify the thermodynamically most stable adsorption state. According to the phase diagram, 0.25ML case would exist more abundant than others within at $300K \leq T \leq 1200K$, 10^{-4} MPa $\leq p \leq 100$ MPa; This conclusion is almost same as chapter 2.4.

Table 2. Energetic and structural properties for

Site	E_{ads} [eV]	H_{avg} [Å]	δ [Å]
0.25ML			
Top	-1.60	2.83	0.160
Bridge	-1.64	2.76	0.055
Hcp	-1.65	2.74	0.083
Fcc	-1.63	2.76	0.067
0.5ML			
Top	-0.90	2.83	0.158
Bridge	-0.94	2.80	0.005
Hcp	-0.97	2.76	0.053
Fcc	-0.96	2.78	0.048
1ML			
Top	-0.60	3.05	0
Bridge	-0.65	2.92	0
Hcp	-0.67	2.88	0
Fcc	-0.66	2.92	0

Table 3. Adsorption energy [eV] of various materials

Surface	E_{ads}	Ref
Ti(0001)	-1.65	
Co(0001)	-1.64	[20]
Rh(111)	-1.89	[31]
Pt(111)	-2.48	[29]

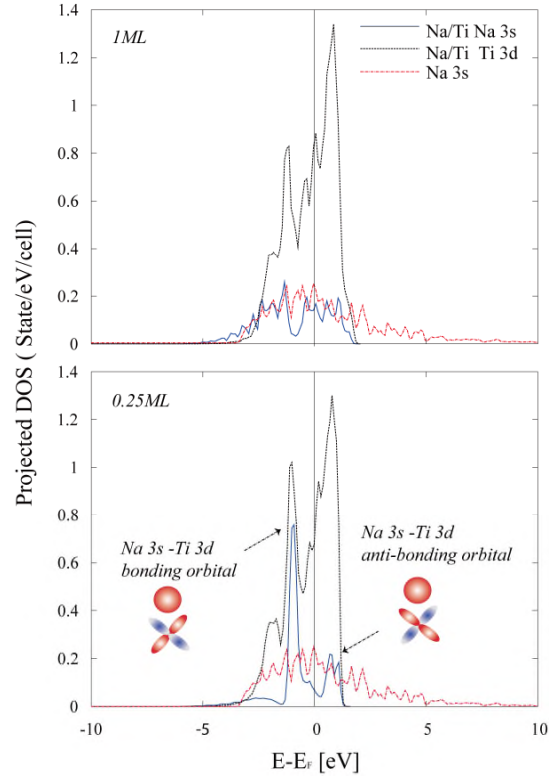


Fig.2 Projected density of states on Ti 3d, Na 3s states for Na on hcp hollow site (1ML,0.25ML) and bulk Na 3s state.

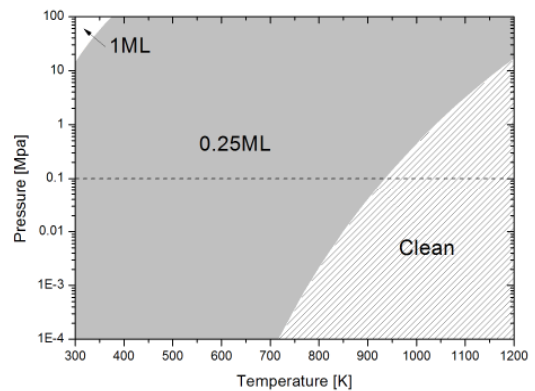


Fig.3 Phase diagram of Na adsorption state at (T,P)

3. Chemisorption effect on the SWR reactivity

In order to model chemisorption effect on the SWR reactivity, basic understanding about SWR kinetics itself should be delivered first; base on the SWR kinetic study and the results at chapter 2, a first trial model of

the reactivity reduction was modeled. Due to the parameters in speculation, the model was incomplete; the validation was done with only 2 experiment cases.

3.1 Fundamentals of SWR kinetics

SWR has been a showcase example which shows extreme reactivity of the alkali metals however, a less study has been conducted due to the application of the SWR is rare. At 1998, Bewig et al.[34] conducted crossed molecular beam experiments, and found NaOH was not made within single collision between Na and H₂O molecules. After this unexpected and surprising experiment results, a several studies has been conducted to understand the kinetics of SWR[34–41]through molecular beam experiments and numerical simulations such as Ab-initio calculation.

Table 4. summarized the history of the studies and the conclusions of kinetic studies of the SWR is as follows.

1. Delocalization of the 3s electron of Na occurs during the initial stage of the SWR; the number of H₂O molecules is a key factor for its stability.
2. The OH bond breaking stage is the rate-limiting step of the reaction; breaking of this bond seems to require several collision with Na atoms.
3. Finally, SWR can be decomposed of 4 steps below.
 1. Na + (H₂O)_n → Na(H₂O)_n
 2. Na + Na → Na₂
 3. Na₂ + Na(H₂O)_n → Na₃(H₂O)_n
 4. Na₃(H₂O)_n → Na + 2NaOH + (n-2)H₂O + H₂

Step 4 was conjectured that the rate limiting step[40] and if step 1,2 and 3 quickly go equilibrium state, H₂ generation rate can be assume to be

$$\frac{d[H_2]}{dt} = K_1 K_2 K_3 k_4 [Na]^3 [H_2O]^n \quad (16)$$

where K₁, K₂ and K₃ are the equilibrium constants for steps 1 – 3 respectively, and k₄ is the reaction rate constant for step 4; n is the reaction order of H₂O.

3.2 SWR reactivity reduction model

The mechanism of SWR reactivity regression can be summarized (Fig 2). Without Ti NPs, H₂ is dominantly generated at the reaction surface (path 1). Some of Na atoms which leave the surface and diffuse into H₂O and react with H₂O (path 2).

The Arrhenius equation can be used to how H₂ generation rate is affected by temperature T, activation energy E_{a,12}, and the number of moles of H₂O and Na at the reaction surface:

$$\frac{d[H_2]}{dt} = f_{1,2}(T, E_{a,1,2}, [H_2O]) \cdot [Na]^3 \quad (17)$$

With Ti NPs, the other reaction path can be assumed as path 3 which is H₂ generation through SWR by adsorbed Na. Like as without Ti NPs, H₂ generation rate will be a function of T, activation barrier of the reaction 1,2 E_{a,12}, activation barrier of the reaction 3 E_{a,3} and

mole of H₂O, Na and Ti NP. β' is the reaction order of Na which is adsorbed onto Ti NPs, however it is hard to estimate due to no studied conducted yet.

$$\frac{d[H_2]}{dt} = f_{1,2}(T, E_{a,1,2}, [H_2O]) [Na - \alpha_1 \alpha_2 NP]^3 + f_3(T, E_{a,3}, [H_2O]) [\alpha_1 \alpha_2 NP]^{\beta'} \quad (18)$$

To estimate the number of Na atoms adsorbed onto NP, α₁ and α₂ are used; α₁ is the ratio of number of adsorbed Na to number of Ti atoms on the NP surface and α₂ is the ratio of number of Ti atoms on the NP surface to the number of NPs. From the result in chapter 3, α₁ is a function of T and P, and is 0.25 in most conditions. Assuming the total number of Ti atoms per volume is constant, α₂ can be a ratio of outmost shell volume to total volume of NP.

$$\alpha_2 = \left(\frac{R_{NP}^3 - (R_{NP} - D_{Ti})^3}{R_{NP}^3} \right) \cdot N_{Ti}^{NP} \quad (19)$$

$$N_{Ti}^{NP} = \frac{4}{3} \pi R_{NP}^3 \cdot \frac{6}{V_{unit,HCP}} \quad (20)$$

where R_{NP} is the radius of the NP, D_{Ti} is the diameter of a Ti atom, N_{TiNP} is the total number of Ti atoms in NP, and V_{unit,HCP} is the unit volume of Ti metal lattice structure (HCP).

Until non-adsorbed Na atoms are exist enough, H₂ generation is occurred through non-adsorbed Na dominantly. However, if Na-αNP ≤ 0, H₂ generation rate will be occurred through the adsorbed Na and H₂ generation rate will be like as follows.

$$\frac{d[H_2]}{dt} = f_3(T, E_{a,3}, [H_2O]) [\alpha_1 \alpha_2 NP]^{\beta'} \quad (21)$$

The reactivity regression rate χ between with and without Ti NPs can be defined as follows.

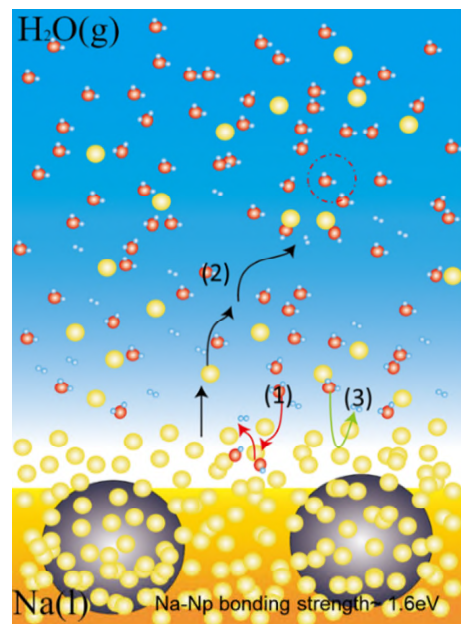


Fig 2. Schematic of SWR with Ti NPs

Table 4. Summary of SWR kinetic studies

Year	Summary	Author
Experiments (Crossed Molecular Beam experiment)		
1998	NaOH will not be made from the single collision of the Na and H ₂ O	L. Bewig et.al.[34]
	Multi collision between (Na) _n and Na(H ₂ O) _m was a necessary step for the reaction products complex of NaOH and H ₂	U.Buck et.al.[35]
2008	Na(H ₂ O) _{3,4} is a dominant product of single collision reaction	Lukasz Cwiklik et al.[38]
Numerical simulations (Ab-initio calculation)		
2000	Na ₂ should be needed to produce NaOH	Christopher J. Mundy et.al.[36]
2005	Na(H ₂ O) _n → NaOH(H ₂ O) _{n-1} +H The activation barrier for this reaction depended on the n.	Ka Wai Chan et al.[37]
2008	After Na collided with (H ₂ O) _{3,4} , 3s electron of Na atom became delocalized between Na ⁺ and H ₂ O molecule, however the complete dissociation of Na ⁺ and delocalized 3s electron was not found.	Lukasz Cwiklik et al.[39]
2009	OH bond breaking reaction was strongly favored in the Na ₃ (H ₂ O) _{6,7} system. NaH formation was suggested a reaction rate limit step.	A V Vorontsov et al.[40]
2013	OH bond breaking reaction in Na(H ₂ O) _n system was initiated by capturing of the hydrated electron from Na by H atoms in H ₂ O molecules nearby Na atom	Kenro Hashimoto et al.[41]

$$\chi \equiv \frac{d[H_2]}{dt}_{1,2,3} / \frac{d[H_2]}{dt}_{1,2} \quad (22)$$

$$= \frac{[Na - \alpha_1 \alpha_2 NP]^3}{[Na]^3} + \frac{f_3(T, E_{a,3}, [H_2O]) \cdot [\alpha_1 \alpha_2 NP]^{\beta'}}{f_{1,2}(T, E_{a,1}, [H_2O]) \cdot [Na]^3}$$

From the results of chapter 2 and 3.1, adsorbed Na cannot easily initiate the SWR; this is because the strong covalent-like metallic bonding between Na and Ti NP surface atom prevents delocalization of Na 3s electrons and multi-collisions of Na atoms which are essential steps in SWR. Therefore E_{a,3} can be assumed to be >> E_{a,12} (f_{1,2} >> f₃), so χ becomes primarily a function of the number of moles of Ti NPs at the reaction surface.

$$\chi = \left[1 - \frac{\alpha_1 \alpha_2 NP}{Na} \right]^{\beta'} \quad (\text{if } f_{1,2} \gg f_3)$$

$$= \left[1 - \alpha_1 \alpha_2 \frac{C_{NP, \text{Interface}} M_{Na}}{1 - C_{NP, \text{Interface}} N_{AV} \left(\frac{4}{3} \pi R_{NP}^3 \right) \rho_{Na}} \right]^{\beta'} \quad (23)$$

This relation is valid only where, Na-αNP > 0. C_{NP,Interface} is function of time and it reached its maximum when (Na-αNP = 0).

$$\text{Max}(C_{NP, \text{Interface}}) = \frac{M_{Na}}{\rho_{Na} \alpha_1 \alpha_2} / \left(1 + \frac{M_{Na}}{\rho_{Na} \alpha_1 \alpha_2} N_{AV} \left(\frac{4}{3} \pi R_{NP}^3 \right) \right) \quad (24)$$

If Na-αNP ≤ 0, so non-adsorbed Na is fully consumed by SWR, χ becomes as follows because SWR can be occurred by adsorbed Na.

$$\chi = \frac{f_3(T, E_{a,3}, [H_2O]) \cdot [\alpha_1 \alpha_2 NP]^{\beta'}}{f_{1,2}(T, E_{a,1,2}, [H_2O]) \cdot [Na]^3} \quad (25)$$

χ at Na-αNP ≤ 0 can be assumed to have a very low value, however, χ at Na-αNP ≤ 0 cannot be evaluated because f₃, f₁ and β' are unknown.

Fig 3. illustrate Expected H₂ generation rate based on the model. t₁ and t₂ indicate the time when non-adsorbed Na is fully consumed by the SWR without and with Ti NPs respectively.

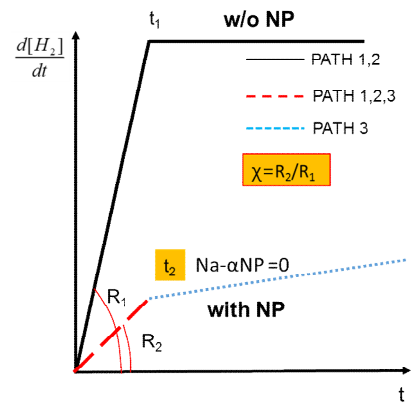


Fig 3. Schematic of [H₂]/dt vs t

3.3 SWR reactivity reduction model implementation

To validate the model and assess its limitations, an analysis of results of previous experiments (Table 5) was conducted. From the data of Saito,J-i et al[6] and Park,G et al[7] experimental data. From the Saito,J-i et al[6]data, at $t < 1s$, average $\chi = 0.921$ and after 1s χ is dramatically reduced to 0.043 and 0.008. From the data of Park,G et al[7]experimental data, χ transition is occurred at $t=4.8s$ and at $t < 4.8s$, $\chi=0.490$; after 4.8s, $\chi=0.490$ is reduced to 0.019. According to the model, these χ transition indicate non-adsorbed or “Ti NPs effect free Na” is fully consumed and dominant reaction path was changed at path 3. Before the transition of χ and SWR perturb the reaction surface remarkably, at the initial, χ can be evaluated by using $C_{NP,Interface}=C_{NP,Bulk}$ at $t=0$. Therefore χ at $t < 1s$ from the experiment results are compared with the value predicted by model. Parameters for model implementation and results are summarized at Table 6 and Fig.4. Square symbols indicate Saito,J-i et al[6] experiment and model prediction data and triangle symbols indicate Park,G.,et al[7] case. Relative error η_{error} is defined like as

$$\eta_{error} = \frac{|\chi - \chi_{model}|}{\chi} \cdot 100 \quad (26)$$

The Model predict Saito,J-i et al[6] experimental data within $\eta_{error}=8\%$ and Park,G et al[7] experimental data within $\eta_{error}=104\%$. The model predict Saito,J-i et al[6] experimental data reasonably well, however Park,G et al[7] is not matched with the model. This discrepancy can be come from the error made in the evaluation of $C_{NP,Interface}$, because $C_{Interface}=C_{NP,bulk}$ assumption can be failed with increasing the NP size; average NP size used in Park,G et al[7] was 5 times larger than Saito,J-i et al[6]. If enough potential barrier was exist at the reaction surface, large size Ti NPs can be adsorbed at the reaction surface and packed each other. Unfortunately, unknown of potential barrier and NPs inter-particle potential make the estimation of the NP packed structure however it can be evaluate by varying $C_{NP,Interface}$ from $C_{NP,bulk}$ to maximum of $C_{NP,Interface}$ evaluated by Eq.23. Fig.5. shows χ variation with respect to $C_{NP,Interface}$ for Park,G.,et al[7] experimental case which is $D_{NP}=50nm$. Dot line indicates the χ value at the experiment and the line cross at $C_{NP,interface}=23.4mM$ This indicate that NP at the reaction surface is packed denser than NP at the liquid Na bulk. When the NP is packed as BCC and FCC, $C_{NP,interface}$ is 13.0mM and 51.987mM respectively. Therefore, NP which has $D_{NP}=50nm$ can be assumed as packed denser than BCC lattice structure but sparser than FCC lattice structure which is mathematically the densest structure. However, this conjecture has no direct evidence such as visualizations and therefore, the model need to be validated with more experiment data with enough accuracy.

Table 5. Previous experiment result, χ

Time region	Saito,J-i.et.al.[6]	Park,G.,et al.[7]
$t_1[s]$	2.3	3
$t_2[s]$	1	4.8
χ at $t < t_2$	0.921	0.490
χ at $t_2 < t$	0.043	0.019

Table 6. Parameters for model implementation and results

	Saito,J-i.et.al.[6]	Park,G.,et al.[7]
D_{NP} [nm]	10	50
T [K]	473	373
α_1	0.25	0.25
α_2	4141.701	108589.552
N_{Ti}	24915	24915337
$C_{NP,bulk}$ [mM/m ³]	28.083	0.0532
$C_{NP,interface}$ at Na- α NP=0[mM/m ³]	2898.721	24.965
χ at $t < t_2$	0.921	0.490
χ_{model} ($C_{NP,interface}=C_{NP,bulk}$)	0.997	1.00
Relative error [%]	8	104

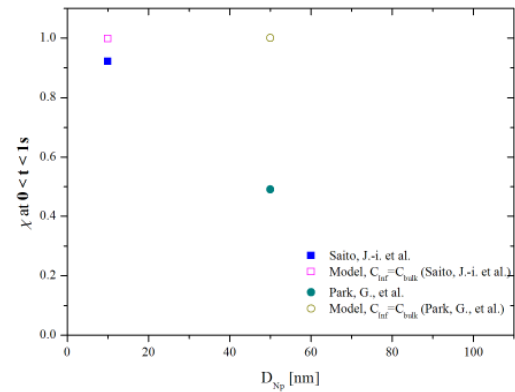


Fig.4. χ ($t < t_2$) vs D_{NP}

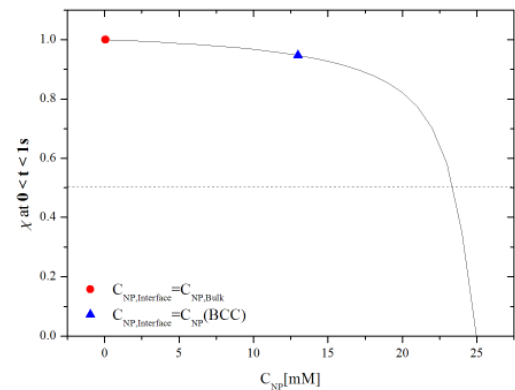


Fig.5. χ vs $C_{NP,Interface}$ (case 2[13]) dotted line indicates experiment results

4. Conclusions

The repression of SWR by Ti NPs was expected to be caused by strong chemical interaction between Ti NP surface and Na atoms; ab initio calculation using density functional theory and atomistic thermodynamic approach were conducted to test this hypothesis. Adsorption of 0.25ML Na at hcp hollow sites was the most favorable adsorption surface state and strong chemical adsorption was confirmed by the adsorption energy of -1.65 eV. A covalent-like metallic bond was confirmed between adsorbed Na and Ti atoms on the Ti(0001) surface; this bond affects the hydration energy of Na atoms and the activation barrier of the SWR. Using adsorption energy from the ab-initio calculation and atomistic thermodynamics, the thermodynamically most stable adsorption state at (T,P) was determined Na chemisorption effect on the SWR reactivity regression rate is modeled. The model predict χ variation with respect to time well especially dramatic reduction of χ ; the χ at $t < 1s$ from Saito, J-i et al[6] experimental data within $\eta_{\text{error}}=8\%$ and Park, G et al[7] experimental data within $\eta_{\text{error}}=104\%$. Large discrepancy between the model and experiment results at Park, G et al[7], can be assumed to the error of $C_{\text{NP,Interface}}$ evaluation. If NP is pecked denser than BCC lattice structure, so $C_{\text{NP,Interface}} = 23.4\text{mM}$ χ discrepancy becomes 0. In order to validate the model, precise experiment results with visualization should be conducted further.

Acknowledgement

This work was supported by the National Research Foundation of Korea (NRF) grant funded by the Korea government (MEST) (NRF-2010-0018679)

Nomenclature

A	Surface area [m ²]
C	NP molar concentration [mole/m ³]
D	Diameter [m]
E	Total energy [J]
F	Helmholtz free energy [J]
f	Force [N]
G	Gibbs free energy [J]
H	Hamiltonian [J]
h	Plank constant (6.63*10 ⁻³⁴ J/s), Nanoparticle immersion depth [m]
K	Equilibrium constant
k	Constrain force constant [J/m]
k _B	Boltzmann constant (1.38*10 ⁻²³ J/K)
N	Total number of (electron, Na)
N _{AV}	Avogadro's number
n	Electron number density [m ⁻³]
Q	Canonical partition function
R	Nuclei coordinate, radius [m]
r	Electron coordinate
S	Entropy

T	Kinetic energy [J]
t	Time [s]
U	Potential energy [J]
V	Volume [m ³]
X	Number of Na adatoms

Greek symbols

α	Coefficient for SWR reactivity regression model
β	Na reaction order for SWR
γ	Surface energy [J/m ²]
δ	Rumpling of Ti atom [m]
ϵ	Kohn-Sham energy
θ	Na surface coverage
ρ	Electron charge density [e/m ³]
Ψ	Nuclear and electron Probability density function
ϕ	Kohn-Sham state
χ	SWR reactivity reduction rate
η	Relative error

Subscript

ads	Adsorption
e	Electron
ext	External potential of Kohn Sham equation
H	Hartree potential, columbic interaction between electrons
i	index for orbital
KS	Kohn and Sham
N-N	interaction between nucleus and nucleus
N-e	interaction between nucleus and electrons
Na/T	Na adsorbed on Ti(0001) surface
i	
xc	exchange-correlation potential of Kohn Sham equation

REFERENCES

- [1] K. Aoto, N. Uto, Y. Sakamoto, T. Ito, M. Toda, S. Kotake, Design study and R&D progress on Japan sodium-cooled fast reactor, J. Nucl. Sci. Technol. 48 (2011) 463–471.
- [2] M. Ichimiya, T. Mizuno, S. Kotake, A next generation sodium-cooled fast reactor concept and its R&D program, Nucl. Eng. Technol. 39 (2007) 171.
- [3] M. Konomura, M. Ichimiya, Design challenges for sodium cooled fast reactors, J. Nucl. Mater. 371 (2007) 250–269.
- [4] K. Ara, K. Sugiyama, H. Kitagawa, M. Nagai, N. Yoshioka, Study on Chemical Reactivity Control of Sodium by Suspended Nanoparticles I, J. Nucl. Sci. Technol. 47 (2010) 1165–1170. <Go to ISI>://WOS:000287013400008.
- [5] J.-I. Saito, K. Nagai, K. Ara, Study on Liquid Sodium with Suspended Nanoparticles-(2) Atomic Interaction and Characteristics of Liquid Sodium with Suspended Nanoparticles, in: AIP Conf. Proc.,

- American Institute of Physics, Ste. 1 NO 1 Melville NY 11747-4502 United States, 2012.
- [6] J. Saito, K. Ara, A study of atomic interaction between suspended nanoparticles and sodium atoms in liquid sodium, *Nucl. Eng. Des.* 240 (2010) 2664–2673. doi:<http://dx.doi.org/10.1016/j.nucengdes.2010.07.017>.
- [7] G. Park, S.J. Kim, M.H. Kim, H.S. Park, Experimental study of the role of nanoparticles in sodium–water reaction, *Nucl. Eng. Des.* 277 (2014) 46–54.
- [8] G. Park, S. Kim, M. Kim, Reduction of chemical reactivity of liquid sodium by Ti nanoparticles, (2013). http://www.kns.org/kns_files/kns/file/13F-01B-3A-%B9%DA%B1%D9%BF%B1.pdf (accessed August 25, 2015).
- [9] G. Park, S. Kim, H. Park, Reaction rate of Na-based titanium nanofluid with water, *J. Nucl.* (2015). <http://www.tandfonline.com/doi/abs/10.1080/00223131.2015.1070767> (accessed August 25, 2015).
- [10] S.J. Kim, G. Park, M.H. Kim, H.S. Park, J. Baek, A theoretical study of Ti nanoparticle effect on sodium water reaction: Using ab initio calculation, *Nucl. Eng. Des.* 281 (2015) 15–21. doi:<http://dx.doi.org/10.1016/j.nucengdes.2014.10.019>.
- [11] J. Saito, T. Itami, K. Ara, The preparation, physicochemical properties, and the cohesive energy of liquid sodium containing titanium nanoparticles, *J. Nanoparticle Res.* 14 (2012). <Go to ISI>://WOS:000312894200040.
- [12] M. Born, R. Oppenheimer, Zur quantentheorie der molekeln, *Ann. Phys.* 389 (1927) 457–484.
- [13] J.C. Slater, The theory of complex spectra, *Phys. Rev.* 34 (1929) 1293.
- [14] P. Hohenberg, W. Kohn, Inhomogeneous electron gas, *Phys. Rev.* 136 (1964) B864.
- [15] W. Kohn, L.J. Sham, Self-consistent equations including exchange and correlation effects, *Phys. Rev.* 140 (1965) A1133.
- [16] P. Giannozzi, S. Baroni, N. Bonini, M. Calandra, R. Car, C. Cavazzoni, et al., QUANTUM ESPRESSO: a modular and open-source software project for quantum simulations of materials, *J. Phys. Condens. Matter.* 21 (2009) 395502.
- [17] D. Vanderbilt, Soft self-consistent pseudopotentials in a generalized eigenvalue formalism, *Phys. Rev. B.* 41 (1990) 7892.
- [18] J.P. Perdew, K. Burke, M. Ernzerhof, Generalized gradient approximation made simple, *Phys. Rev. Lett.* 77 (1996) 3865.
- [19] D.S. Sholl, J.A. Steckel, *Density functional theory: a practical introduction*, Wiley, Hoboken, N.J., 2009. <http://dx.doi.org/10.1002/9780470447710>.
- [20] S.H. Ma, Z.Y. Jiao, T.X. Wang, Z.X. Yang, Density functional study of K and Na adsorbed on Co(0001), *Eur. Phys. J. B.* 75 (2010) 469–474. <Go to ISI>://WOS:000279227500008.
- [21] H.J. Monkhorst, J.D. Pack, Special points for Brillouin-zone integrations, *Phys. Rev. B.* 13 (1976) 5188–5192.
- [22] M. Methfessel, A.T. Paxton, High-precision sampling for Brillouin-zone integration in metals, *Phys. Rev. B.* 40 (1989) 3616.
- [23] K. Hermann, *Crystallography and Surface Structure: An Introduction for Surface Scientists and Nanoscientists*, John Wiley & Sons, 2011.
- [24] P.A. Tipler, *Elementary modern physics*, Macmillan, 1992.
- [25] D. Hahn, Y. Kim, C.B. Lee, S. Kim, J. Lee, Y. Lee, et al., Conceptual design of the sodium-cooled fast reactor KALIMER-600, *Nucl. Eng. Technol.* 39 (2007) 193.
- [26] J. Rogal, K. Reuter, *Ab initio atomistic thermodynamics for surfaces: A primer*, DTIC Document, 2006.
- [27] L.-Y. Gan, R.-Y. Tian, X.-B. Yang, Y.-J. Zhao, Surface structure and phase transition of K adsorption on Au (111): By ab initio atomistic thermodynamics, *J. Chem. Phys.* 136 (2012) 44510.
- [28] D.L. Doering, S. Semancik, Low temperature ordering of sodium overlayers on Ru (001), *Surf. Sci.* 129 (1983) 177–191.
- [29] S. Moré, A.P. Seitsonen, W. Berndt, A.M. Bradshaw, Ordered phases of Na adsorbed on Pt (111): Experiment and theory, *Phys. Rev. B.* 63 (2001) 75406.
- [30] C. Stampfl, J. Neugebauer, M. Scheffler, Alkali-metal adsorption on Al (111) and Al (100), *Surf. Sci.* 307 (1994) 8–15.
- [31] H.Y. Xiao, D.Q. Xie, Density functional study of the adsorption of Na and K on Rh(111), *Surf. Sci.* 553 (2004) 13–22. <Go to ISI>://WOS:000220271500004.
- [32] B. Hammer, J.K. Nørskov, *Theoretical surface science and catalysis - Calculations and concepts*, *Adv. Catal.* Vol 45. 45 (2000) 71–129. <Go to ISI>://WOS:000089180200002.
- [33] B. Hammer, J.K. Nørskov, Why Gold Is the Noblest of All the Metals, *Nature.* 376 (1995) 238–240. <Go to ISI>://WOS:A1995RK33100041.

- [34] L. Bewig, U. Buck, S. Rakowsky, M. Reymann, C. Steinbach, Reactions of sodium clusters with water clusters, *J. Phys. Chem. A.* 102 (1998) 1124–1129.
- [35] U. Buck, C. Steinbach, Formation of Sodium Hydroxide in Multiple Sodium-Water Cluster Collisions, *J. Phys. Chem. A.* 102 (1998) 7333–7336.
- [36] C.J. Mundy, J. Hutter, M. Parrinello, Microsolvation and chemical reactivity of sodium and water clusters, *J. Am. Chem. Soc.* 122 (2000) 4837–4838. <Go to ISI>://WOS:000087118100047.
- [37] K.W. Chan, C.K. Siu, S.Y. Wong, Z.F. Liu, The elimination of a hydrogen atom in Na(H₂O)_n, *J. Chem. Phys.* 123 (2005). <Go to ISI>://WOS:000232206500024.
- [38] L. Cwiklik, U. Buck, W. Kulig, P. Kubisiak, P. Jungwirth, A sodium atom in a large water cluster: Electron delocalization and infrared spectra, *J. Chem. Phys.* 128 (2008) 154306.
- [39] L. Cwiklik, P. Kubisiak, W. Kulig, P. Jungwirth, Reactivity of a sodium atom in vibrationally excited water clusters: An ab initio molecular dynamics study, *Chem. Phys. Lett.* 460 (2008) 112–115. <Go to ISI>://WOS:000257596300023.
- [40] A. V Vorontsov, Y. V Novakovskaya, Reaction of sodium atoms with water clusters, *Phys. Scr.* 80 (2009). <Go to ISI>://WOS:000270388200028.
- [41] K. Hashimoto, S. Ugajin, S. Yoshida, R. Tazawa, A. Sato, Theoretical study of OH-breaking reactions in Na (H₂O)_n clusters, *Chem. Phys.* 419 (2013) 124–130.